Figure S1.

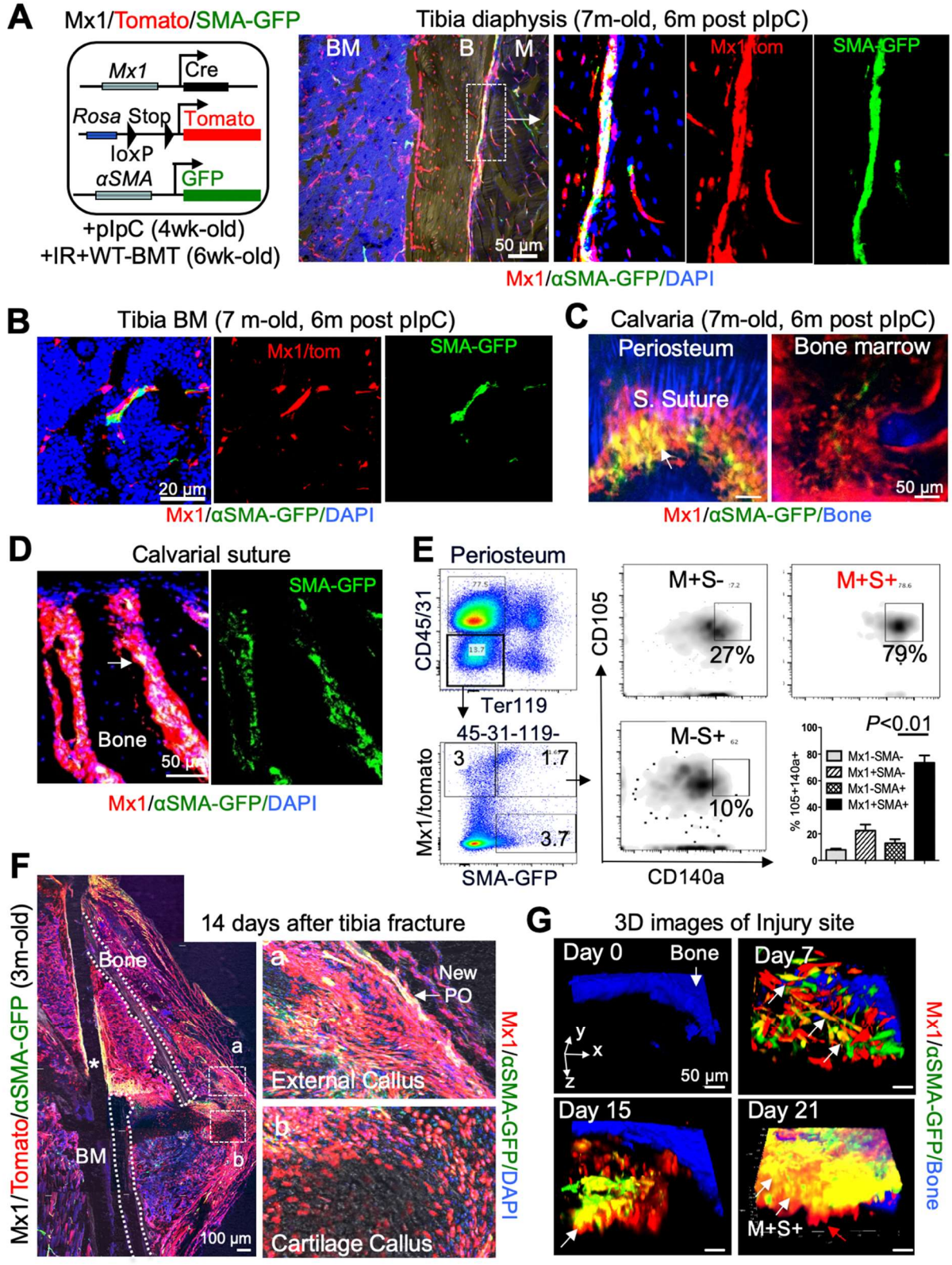
A
Mx1/Tomato/SMA-GFP
Mx1
Cre
Rosa Stop
Tomato
loxP
αSMA
GFP
+pIpC (4wk-old)
+IR+WT-BMT (6wk-old)
Tibia diaphysis (7m-old, 6m post pIpC)
BM
B
M
Mx1/tom
SMA-GFP
50 μm
Mx1/αSMA-GFP/DAPI
B
Tibia BM (7 m-old, 6m post pIpC)
Mx1/tom
SMA-GFP
20 μm
Mx1/αSMA-GFP/DAPI
C
Calvaria (7m-old, 6m post pIpC)
Periosteum
S. Suture
Bone marrow
50 μm
Mx1/αSMA-GFP/Bone
D
Calvarial suture
SMA-GFP
Bone
50 μm
Mx1/αSMA-GFP/DAPI
E
Periosteum
CD45/31
Ter119
45-31-119-
Mx1/tomato
SMA-GFP
CD105
CD140a
M+S-
27%
M+S+
79%
M-S+
10%
P<0.01
% 105+140a+
Mx1-SMA-
Mx1+SMA-
Mx1-SMA+
Mx1+SMA+
F
Mx1/Tomato/αSMA-GFP (3m-old)
14 days after tibia fracture
Bone
BM
100 μm
a
b
New PO
External Callus
Cartilage Callus
Mx1/αSMA-GFP/DAPI
G
3D images of Injury site
Day 0
Bone
Day 7
Day 15
Day 21
M+S+
50 μm
Mx1/αSMA-GFP/Bone

Figure S1. *Mx1*$^+$*αSMA*$^+$ cells are localized to the periosteum and highly express SSPC markers, related to Figure 1. To induce *Mx1* labeling (red), 4-week old Mx1/Tomato/αSMA-GFP dual reporter mice were treated with 5 doses (10 days) of pIpC. Two weeks later, mice were lethally irradiated and underwent wild-type bone marrow transplantation (WT-BMT). The analysis was performed at least 1 month after WT-BMT. **A.** The periosteal *Mx1*$^+$*αSMA*$^+$ population in the tibia of 7-month old Mx1/Tomato/αSMA-GFP dual reporter mice (6 months post pIpC) was analyzed by anti-GFP immunofluorescence staining for enhancing GFP signals. White box indicates periosteal *Mx1*$^+$*αSMA*$^+$ cells (red and green). Right image panels are single channel (Tomato or GFP) images of boxed area. DAPI: Blue; M: muscle; B: bone; BM: bone marrow. Data represent more than five independent experiments. **B.** Bone marrow *Mx1*$^+$ cells (Tomato$^+$) that are distinct from *αSMA*$^+$ cells (GFP$^+$) were assessed by anti-GFP immunofluorescence staining of tibial bone marrow of Mx1/Tomato/αSMA-GFP mice from A. **C & D.** The *Mx1*$^+$*αSMA*$^+$ population in the calvarial suture of Mx1/Tomato/αSMA-GFP dual reporter mice was analyzed by intravital microscopy (**C**) and anti-GFP immunofluorescence staining (**D**). White Arrow (D) indicate *Mx1*$^+$*αSMA*$^+$ cells (Tomato$^+$GFP$^+$) in the calvarial suture. **E.** The periosteal *Mx1*$^+$*αSMA*$^+$ cell population highly expresses SSC-specific markers CD105 and CD140a. Graph shows percentages of the CD105$^+$CD140a$^+$ SSC population within *Mx1*$^+$*αSMA*$^+$, *αSMA*$^+$, or *Mx1*$^+$ cells from the periosteum as determined by flow cytometry (n=6). **F.** 14 days after transverse tibial fracture, robust contribution of the *Mx1*$^+$ (Tomato$^+$) periosteal cells to the external callus (box a), repopulation of *Mx1*$^+$*αSMA*$^+$ (Tomato$^+$GFP$^+$) cells in the new periosteum (white arrow, New PO), and their contribution to cartilaginous callus (box b) were assessed by immunostaining with anti-GFP antibody. Intermedullary pin insertion (*), fractured bone (dot lines) and BM are indicated (n=5). **G**. 3-D reconstruction of *in vivo* z-stack images of the injury site shown in Fig. 1F. *Mx1*$^+$*αSMA*$^+$ cells (arrows) newly appear at the injury site by day 7. By day 21 the injury is filled with more differentiated *Mx1*$^+$*αSMA*$^-$ cells (red arrow), while *Mx1*$^+$*αSMA*$^+$ P-SSCs (white arrow) mainly reside in the outer surface of the injury (representative of 5 independent experiments).

Figure S2.

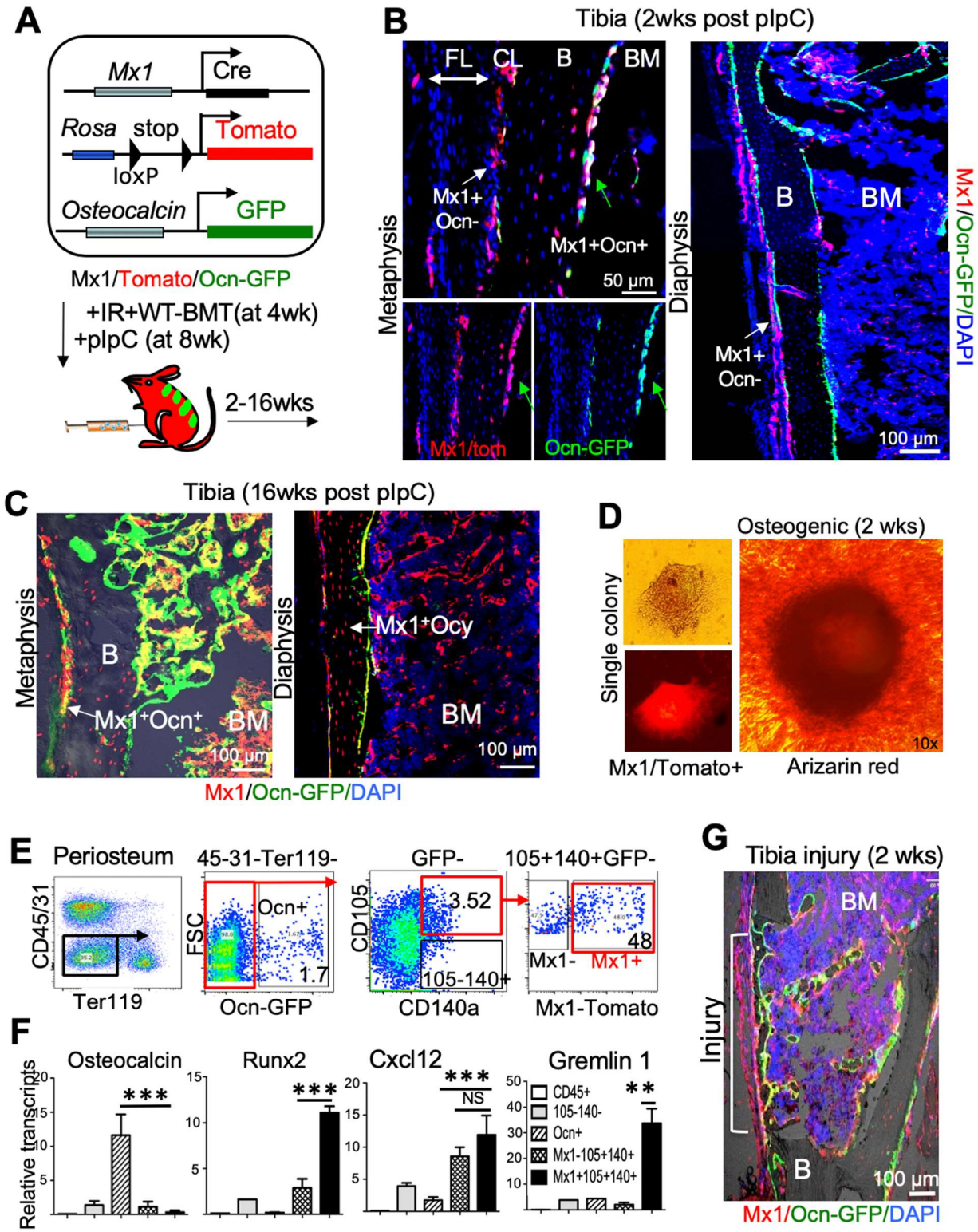
A
Mx1
Cre
Rosa
stop
Tomato
loxP
Osteocalcin
GFP
Mx1/Tomato/Ocn-GFP
+IR+WT-BMT(at 4wk)
+pIpC (at 8wk)
2-16wks
B
Tibia (2wks post pIpC)
FL
CL
B
BM
Metaphysis
Diaphysis
Mx1+
Ocn-
Mx1+Ocn+
50 μm
Mx1/tom
Ocn-GFP
100 μm
Mx1/Ocn-GFP/DAPI
C
Tibia (16wks post pIpC)
Metaphysis
B
Mx1+Ocn+
BM
100 μm
Diaphysis
Mx1+Ocy
Mx1/Ocn-GFP/DAPI
D
Osteogenic (2 wks)
Single colony
10x
Mx1/Tomato+
Arizarin red
E
Periosteum
CD45/31
Ter119
45-31-Ter119-
FSC
Ocn+
1.7
Ocn-GFP
GFP-
CD105
3.52
105-140+
CD140a
105+140+GFP-
Mx1-
Mx1+
48
Mx1-Tomato
F
Osteocalcin
Runx2
Cxcl12
Gremlin 1
Relative transcripts
***
***
***
NS
**
CD45+
105-140-
Ocn+
Mx1-105+140+
Mx1+105+140+
G
Tibia injury (2 wks)
BM
Injury
B
100 μm
Mx1/Ocn-GFP/DAPI

Figure S2. *Mx1*$^+$ periosteal cells are clonogenic progenitors responsible for callus-forming cells *in vivo*, related to Figure 2. A. Schematic representation of *Mx1*-Cre$^+$ *Rosa26*-Tomato$^+$*osteocalcin*-GFP$^+$ mice. Four-week-old Mx1/Tomato/Ocn-GFP dual reporter mice were lethally irradiated and underwent WT-BMT to reduce the background of hematopoietic lineage cells. *Mx1*-Cre was induced at 2 months of age in Mx1/Tomato/Ocn-GFP mice with 5 doses (10 days) of pIpC. **B.** Tibia sections of Mx1/Tomato/Ocn-GFP mice two weeks after pIpC treatment show that most periosteal *Mx1*$^+$ cells are undifferentiated (*Mx1*$^+$*Ocn*$^-$) and reside in the inner cambium layer (CL), rather than the fibrous layer (FL). Differentiated osteoblasts (*Mx1*$^+$*Ocn*$^+$, red and green) in the endosteal surface are indicated by green arrows (n=5). **C.** Increase in *Mx1*$^+$ progenitor contribution to the periosteal osteoblasts and osteocytes (right bottom) over time. 16 weeks after pIpC induction, newly differentiated osteoblasts (*Mx1*$^+$*Ocn*$^+$: red and green) and osteocytes (*Mx1*$^+$ Ocy) from *Mx1*$^+$ periosteal progenitor cells in the periosteum and endosteum of Mx1/Tomato/Ocn-GFP mice (~6-month old, 16 weeks post-pIpC) were analyzed by anti-GFP immunofluorescent staining (n=3). **D.** After induction of *Mx1* with pIpC and WT-BMT, single cell cultures of *Mx1*$^+$ periosteal cells (red) displayed colony formation. Cells from single colony were further incubated in osteogenic medium for 28 days and stained with Alizarin Red. **E & F.** *Mx1*$^+$ progenitors in the periosteum show SSC characteristics. Hematopoietic cells (CD45$^+$), bone marrow stromal cells (CD105$^-$CD140$^+$), osteoblasts (Ocn$^+$), *Mx1*$^-$ and *Mx1*$^+$ SSCs from Mx1/Tomato/Ocn-GFP mouse bones were sorted, and the levels of the indicated genes were quantified by qRT-PCR. ** P<0.01; ***P<0.001. **G.** Robust contribution of *Mx1*$^+$ periosteal progenitors (red) to the majority of new periosteal cells and callus-forming osteoblasts (red and green), without detectable responses of *Mx1*$^+$ bone marrow cells (tomato) 2 weeks after proximal tibial injury. Bone (B) and bone marrow (BM) are indicated. Blue, DAPI (B, C, G). Data represent at least 3-5 mice per group (A-C).

Figure S3.

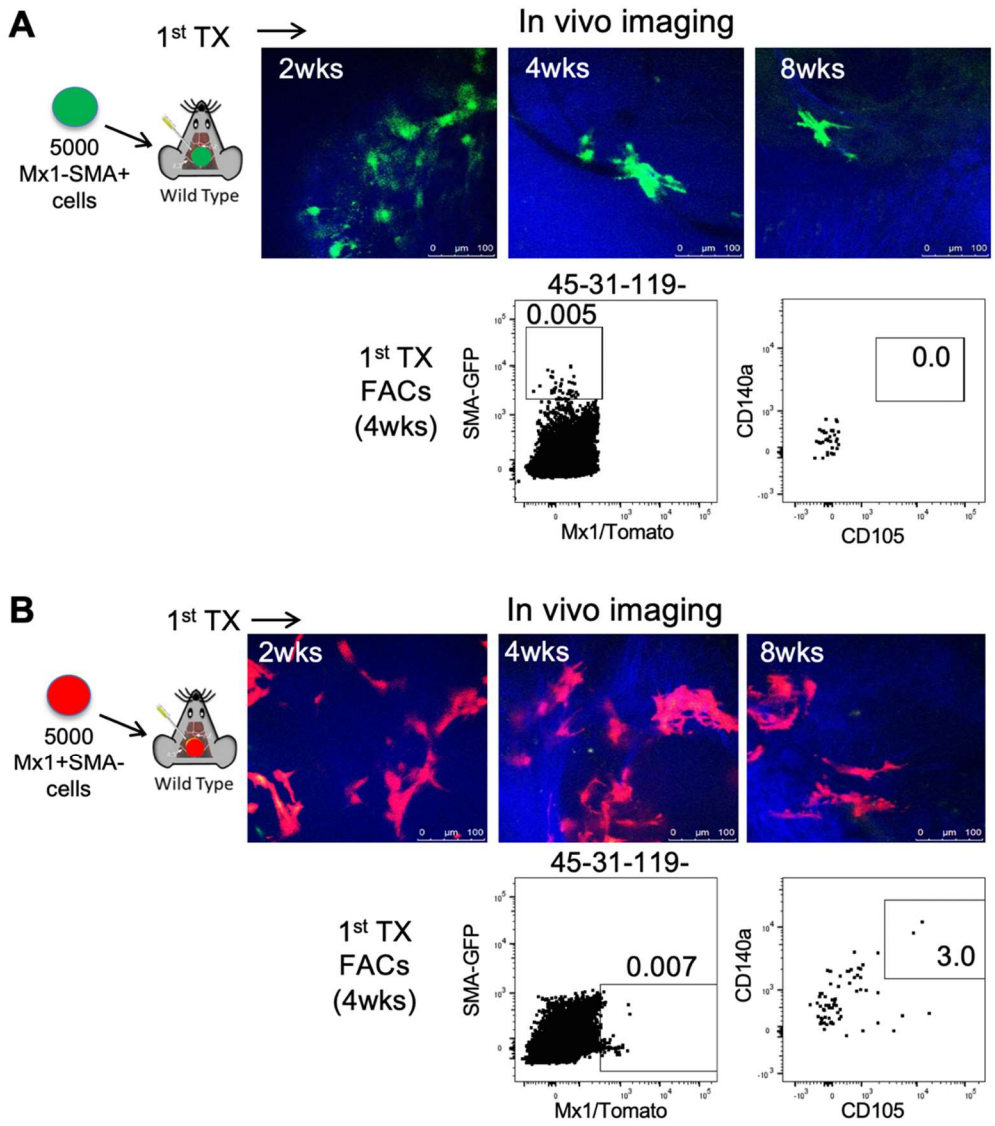

Figure S3. Periosteal cell transplantation related to Figure 3C. Mx1/Tomato/αSMA-GFP dual reporter mice were treated with 5 doses of pIpC every other day to induce *Mx1* labeling (red) at 4 weeks of age, followed by lethal irradiation and WT-BMT. Periosteal cells from 10-12-week old Mx1/Tomato/αSMA-GFP mice were FACs-sorted for $CD45^{-}CD31^{-}Ter119^{-}CD105^{+}CD140^{+}$*Mx1*$^{+}$*αSMA*$^{-}$ (*Mx1*$^{+}$*αSMA*$^{-}$) and $CD45^{-}CD31^{-}Ter119^{-}CD105^{+}CD140^{+}$*Mx1*$^{-}$*αSMA*$^{+}$ (*Mx1*$^{-}$*αSMA*$^{+}$) cell populations. Approximately 5,000 *Mx1*$^{-}$*αSMA*$^{+}$ (**A**) or *Mx1*$^{+}$*αSMA*$^{-}$ (**B**) cells were transplanted onto calvarial injury sites of wild-type C57BL/6 mice. Transplanted cells were then tracked using intravital microscopy 2, 4, and 8 weeks post transplantation. Four weeks after transplantation, transplanted cells were FACs-analyzed for SSC markers (CD105 and CD140a). Data represent five independent transplants per group with comparable results.

Figure S4.

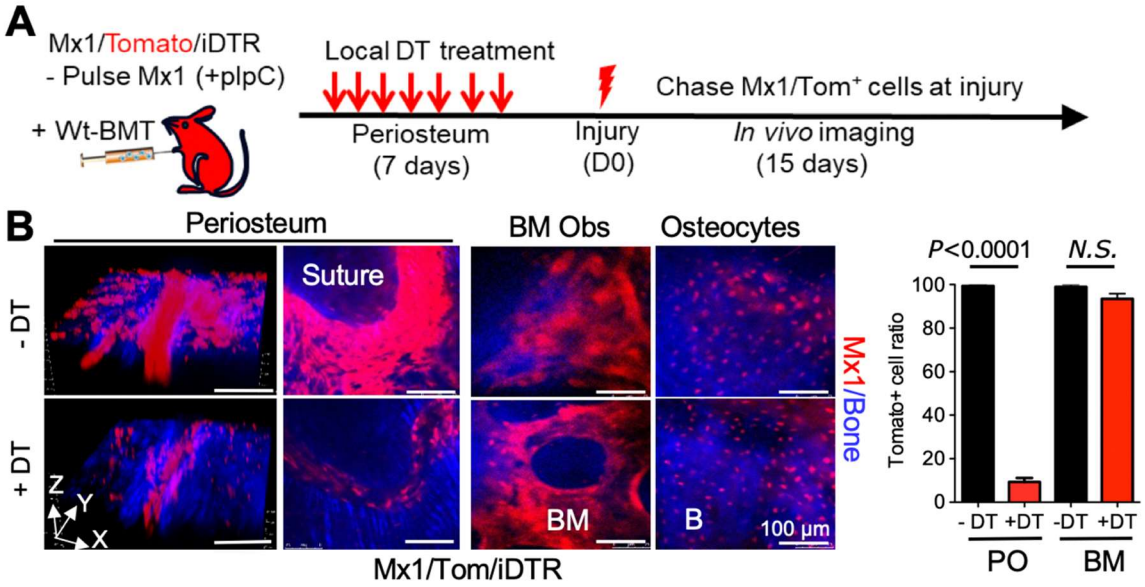

Figure S4. *Mx1*$^{+}$ P-SSCs are necessary for bone healing, related to Figure 3D. A. The periosteum of 10-12-week old *Mx1*/Tomato/iDTR mice (pIpC at 4 weeks of age and WT-BMT at 6 weeks of age) was treated locally with a low-dose of diphtheria toxin (+DT; 20 μL at 1 μg/mL) or control (-DT; PBS) for seven days to ablate *Mx1*$^{+}$ (Tomato^{+}) periosteal cells, but not bone marrow cells. **B.** Local ablation of *Mx1*$^{+}$ periosteal cells. The DT-mediated reduction of the *Mx1*$^{+}$ (Tomato^{+}) populations in the periosteum (PO), without change of *Mx1*$^{+}$ cells in the bone marrow (BM) or osteocytes within the bone, was analyzed by *in vivo* imaging. Data represent at least three independent experiments with comparable results. Scale bar, 100 μm.

Figure S5.

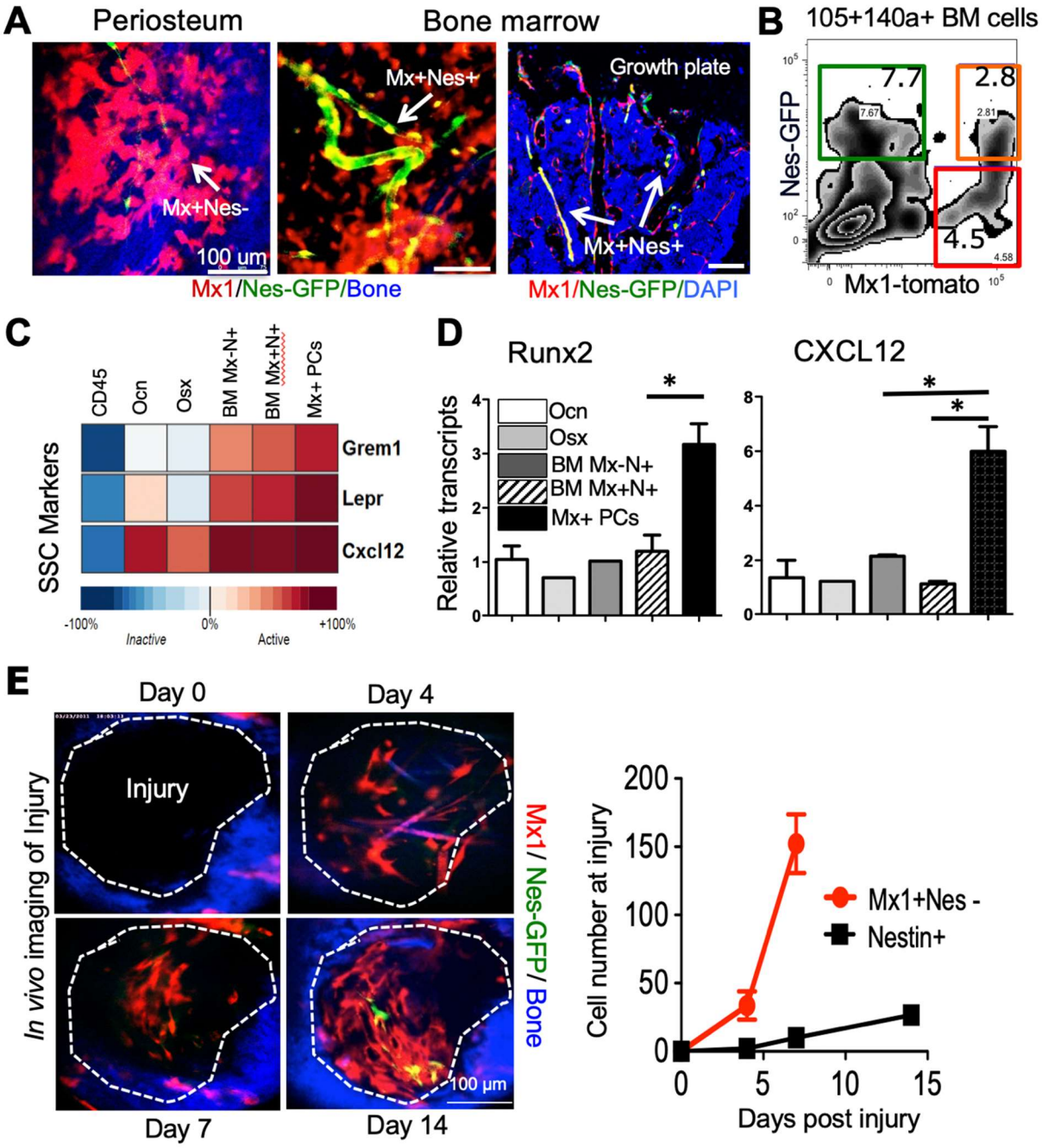
A
Periosteum
Bone marrow
Mx+Nes-
100 um
Mx+Nes+
Growth plate
Mx+Nes+
Mx1/Nes-GFP/Bone
Mx1/Nes-GFP/DAPI
B
105+140a+ BM cells
7.7
2.8
4.5
Nes-GFP
Mx1-tomato
C
CD45
Ocn
Osx
BM Mx-N+
BM Mx+N+
Mx+ PCs
SSC Markers
Grem1
Lepr
Cxcl12
-100%
0%
+100%
Inactive
Active
D
Runx2
CXCL12
Relative transcripts
Ocn
Osx
BM Mx-N+
BM Mx+N+
Mx+ PCs
E
Day 0
Day 4
Day 7
Day 14
Injury
In vivo imaging of Injury
Mx1/ Nes-GFP/ Bone
100 µm
Cell number at injury
Mx1+Nes -
Nestin+
Days post injury

Figure S5. *Mx1*$^+$ periosteal cells distinct from *Nestin*$^+$ BM-SSCs supply new osteoblasts in fracture healing, related to Figure 4B & C. A. Representative *in vivo* image of the periosteum (left) and bone marrow perivascular cells (middle), and an immunofluorescence image of a tibia section (right) from 10-12-weeks old Mx1/Tomato/Nestin-GFP mice (8 weeks after pIpC and WT-BMT) (n>5). **B.** The percentages of *Mx1*$^+$*Nestin*$^+$, *Nestin*$^+$, or *Mx1*$^+$ skeletal progenitors in CD45$^-$CD31$^-$Ter119$^-$CD105$^+$CD140$^+$ cells from Mx1/Tomato/Nestin-GFP bones were determined by flow cytometry (n>5). **C & D.** CD45$^+$ hematopoietic cells (CD45), GFP$^+$ cells from *Osteocalcin*-GFP mice (Ocn), GFP$^+$ cells from *Osterix*-GFP mice (Osx), and *Mx1*$^-$*Nestin*$^+$ (BM Mx-N+) and *Mx1*$^+$*Nestin*$^+$ (BM Mx+N+) cells within the CD45$^-$CD31$^-$Ter119$^-$CD105$^+$CD140a$^+$ population from Mx1/Tomato/Nestin-GFP mouse bone marrow (BM) and *Mx1*$^+$*Ocn*$^-$ periosteal cells (*Mx1*$^+$ PCs) within the CD45$^-$CD31$^-$Ter119$^-$CD105$^+$CD140a$^+$ population from Mx1/Tomato/Ocn-GFP mice were sorted. Heatmaps **(C)** represent the relative gene expression levels of SSC markers compared with ~10,000 public microarray datasets (global-scale meta-analysis with Gene Expression Commons). The relative expression level of SSC markers (**D,** Runx2 and Cxcl12) in the indicated cells was analyzed by RT-PCR (n=5 per group). * P<0.05. **E.** *Mx1*$^+$ SSCs, but not *Nestin*-GFP$^+$ cells, supply the majority of osteoblasts in fracture healing. *Mx1*$^+$ (Tomato$^+$) and *Nestin*-GFP$^+$ cells near the injury site on calvaria of Mx1/Tomato/Nestin-GFP mice were imaged at the indicated times after injury.

Figure S7

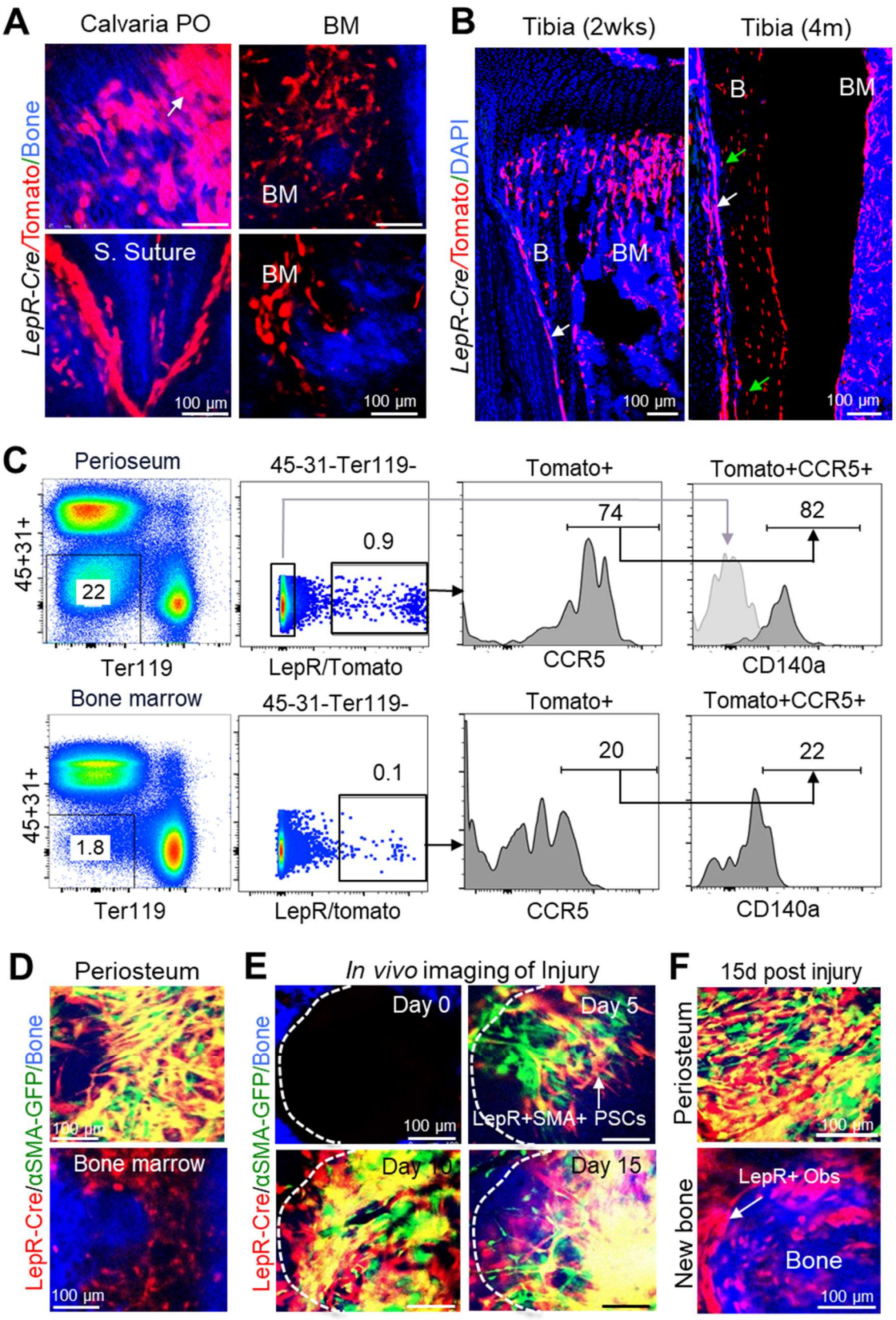
A
Calvaria PO
BM
LepR-Cre/Tomato/Bone
S. Suture
BM
BM
100 μm
100 μm
B
Tibia (2wks)
Tibia (4m)
LepR-Cre/Tomato/DAPI
B
BM
B
BM
100 μm
100 μm
C
Perioseum
45-31-Ter119-
Tomato+
Tomato+CCR5+
45+31+
22
0.9
74
82
Ter119
LepR/Tomato
CCR5
CD140a
Bone marrow
45-31-Ter119-
Tomato+
Tomato+CCR5+
45+31+
1.8
0.1
20
22
Ter119
LepR/tomato
CCR5
CD140a
D
Periosteum
LepR-Cre/αSMA-GFP/Bone
100 μm
Bone marrow
100 μm
E
In vivo imaging of Injury
LepR-Cre/αSMA-GFP/Bone
Day 0
100 μm
Day 5
LepR+SMA+ PSCs
Day 10
Day 15
F
15d post injury
Periosteum
100 μm
New bone
LepR+ Obs
Bone
100 μm

Figure S6. *LepR*$^+$ periosteal cells are distinct from *LepR*$^+$ bone marrow cells and supply new osteoblasts in fracture healing, related to Figure 4. A. *In vivo* imaging of *LepR*-Cre$^+$*Rosa26*-Tomato$^+$ reporter mice. ***LepR*$^+$** (Tomato$^+$) cells are present in the periosteum, sutures, and bone marrow (BM) of the calvaria. **B.** Representative tibia sections from 2-week old and 4-month old LepR/Tomato mice showing distinct *LepR*$^+$ progenitor cells (white arrows) present in the periosteum and their increasing contribution to *LepR*$^+$ osteocytes (4m, green arrows) with age. Bone (B), and bone marrow (BM). Blue, DAPI. **C.** CCR5 and CD140a expression of ***LepR*$^+$** cells isolated from the periosteum (top) or bone marrow (bottom) was analyzed by flow cytometry (n>5). **D.** Selective labeling of *LepR*$^+$*αSMA*$^+$ cells in the periosteum was assessed by *in vivo* imaging of calvarial periosteum and the underneath bone marrow of 10-12-week old LepR/Tomato/αSMA-GFP dual reporter mice. **E.** Sequential *in vivo* imaging of *LepR*$^+$ (Tomato$^+$), *αSMA*$^+$ (GFP$^+$), and *LepR*$^+$*αSMA*$^+$ (Tomato$^+$GFP$^+$) cells in response to a calvarial injury on days 0, 4, 7, and 12 post-injury. Arrow (day 5) indicates migrating and/or proliferating *LepR*$^+$α*SMA*$^+$ periosteal cells near the injury site. Blue, bone. **F.** Fifteen days after injury, *LepR*$^+$*αSMA*$^+$ cells are abundant on the regenerating periosteum (top image), contributing to the majority of bone-forming osteoblasts (*LepR*$^+$ Obs) within the newly formed bone at the injury site (blue; bottom image).

Table S1. Primer sequences for RT-qPCR related to STAR Methods

Gene	Primer Bank ID	Sequence
GAPDH-F	NM-001012477	CGCCAAGGTCGTCGCCG
GAPDH-R	NM-008084	TGTGTCCGTCGTGGATCTGA
Runx2-F	NM-001146038	TTCAACGATCTGAGATTTGTGGG
Runx2-R	NM-001146038	GGATGAGGAATGCGCCCTA
Osteocalcin-F	NM-031368	CTGACCTCACAGATCCCAAGC
Osteocalcin-R	NM-031368	TGGTCTGATAGCTCGTCACAAG
CXCL12-F	NM-001012477	CGCCAAGGTCGTCGCCG
CXCL12-R	NM-013655	TTGGCTCTGGCGATGTGGC
LepR-F	NM-146146	GTCTTCGGGGATGTGAATGTC
LepR-R	NM-146146	ACCTAAGGGTGGATCGGGTTT
Gremlin-F	NM-146007	GCTCTCCTTCGTCTTCCTC
Gremlin-R	NM-146007	AGTGTATGCGGTGCGATTC